Oncostatin M-stimulated apical plasma membrane biogenesis requires p27(Kip1)-regulated cell cycle dynamics

Van IJzendoorn, Sven C D; Théard, Delphine; Van Der Wouden, Johanna M; Visser, Willy; Wojtal, Kacper A; Hoekstra, Dick

Published in:
Molecular Biology of the Cell

DOI:
10.1091/mbc.E04-03-0201

Molecular Biology of the Cell
Vol. 15, 4105–4114, September 2004

Oncostatin M-stimulated Apical Plasma Membrane Biogenesis Requires $p27^{Kip1}$-Regulated Cell Cycle Dynamics

Sven C.D. van IJzendoorn,*† Delphine Théard,* Johanna M. van der Wouden, Willy Visser, Kacper A. Wojtal, and Dick Hoekstra

Department of Membrane Cell Biology, University of Groningen, 9713 AV, Groningen, The Netherlands

Submitted March 11, 2004; Revised June 17, 2004; Accepted June 24, 2004
Monitoring Editor: Keith Mostov

Oncostatin M regulates membrane traffic and stimulates apicalization of the cell surface in hepatoma cells in a protein kinase A-dependent manner. Here, we show that oncostatin M enhances the expression of the cyclin-dependent kinase (cdk)2 inhibitor $p27^{Kip1}$, which inhibits G_1-S phase progression. Forced G_1-S-phase transition effectively renders presynchronized cells insensitive to the apicalization-stimulating effect of oncostatin M. G_1-S-phase transition prevents oncostatin M-mediated recruitment of protein kinase A to the centrosomal region and precludes the oncostatin M-mediated activation of a protein kinase A-dependent transport route to the apical surface, which exits the subapical compartment (SAC). This transport route has previously been shown to be crucial for apical plasma membrane biogenesis. Together, our data indicate that oncostatin M-stimulated apicalization of the cell surface is critically dependent on the ability of oncostatin M to control $p27^{Kip1}$/cdk2-mediated G_1-S-phase progression and suggest that the regulation of apical plasma membrane-directed traffic from SAC is coupled to centrosome-associated signaling pathways.

INTRODUCTION

The establishment and maintenance of apical and basolateral plasma membrane (PM) domains in epithelia require a careful orchestration of extra- and intracellular signals, triggering crucial cytoskeleton-, organelle-, and membrane traffic-linked machineries, as partly elucidated in systems as diverse as yeast, *Drosophila*, and mammalian cells (Lecuit and Pilot, 2003; Mostov *et al*., 2003; Baas *et al*., 2004). Impairment of these events may cause a loss of apical-basolateral asymmetry and may lead to deranged cell growth (Bilder *et al*., 2000; Vermeer *et al*., 2003; Baas *et al*., 2004) or spindle misorientation (Albertson and Doe, 2003). Recent studies have reported an evolutionary conserved genetic program that may link the process of polarity development and proliferation (Bilder *et al*., 2000; Humbert *et al*., 2003; Rolls *et al*., 2003; Klezovitch *et al*., 2004). However, many aspects of such a link remain unclear, e.g., the extent to which cell proliferation can directly affect epithelial cell organization or vice versa. Indeed, epithelial cell proliferation and apical-basolateral polarity may be controlled by different signaling pathways (Liu *et al*., 2004).

Signaling cascades stimulated by interleukin-6 family cytokines, including oncostatin M (OSM), elicit multiple responses in the cell. Originally, as its name indicates, oncostatin M was primarily recognized to inhibit the proliferation of tumor cells (Tanaka and Miyajima, 2003), presumably by modulating cell cycle regulatory proteins, including the cyclin-dependent kinase (cdk)2-inhibitor $p27^{Kip1}$ (Kortylewski *et al*., 1999; Klausen *et al*., 2000; Li *et al*., 2001). Disruption of the regulatory system that controls G_1-phase progression is a common event in human hepatocarcinogenesis (Hui *et al*., 1998), and $p27^{Kip1}$ has been associated with differentiation, invasiveness, and metastasis of hepatocellular carcinoma tumors (Zhou *et al*., 2003). Recent evidence indicate that OSM signaling plays a prominent role in liver development (Kamiya *et al*., 1999, 2001, 2002; Kojima *et al*., 2000; Kinoshita and Miyajima, 2002; Matsui *et al*., 2002; Chagraoui *et al*., 2003; Hanada *et al*., 2003; Lazaro *et al*., 2003). OSM stimulates hepatocyte nuclear factor-4 (Kamiya *et al*., 2003), which may integrate the genetic programs of liver-specific gene expression and epithelial morphogenesis (Spath and Weiss, 1998). In addition, OSM induces adherens junction formation by altering the subcellular localization of adherens junction components, including E-cadherin and catenins (Matsui *et al*., 2002). In human fetal hepatocytes as well as in well-differentiated human hepatic HepG2 cells, OSM stimulates the development of apical bile canalicular plasma membrane (PM) domains (Lazaro *et al*., 2003; van der Wouden *et al*., 2002), which requires the activation of a gp130-mediated signaling cascade and endogenous protein kinase A (PKA) activity (van der Wouden *et al*., 2002). Although the molecular mechanisms that underlie apicalization of the cell surface in hepatocytes are poorly understood, the de novo reorganization of the lateral PM after the establishment of E-cadherin–dependent cell-cell adhesion, mediated by cytoskeleton rearrangements and the polarized sorting and trafficking of proteins and lipids, plays a crucial role.

Article published online ahead of print. Mol. Biol. Cell 10.1091/mbc.E04–03–0201. Article and publication date are available at www.molbiolcell.org/cgi/doi/10.1091/mbc.E04–03–0201.

* These authors contributed equally to this work.

† Corresponding author. E-mail address: s.c.d.van.ijzendoorn@med.rug.nl.

Apical protein and lipid sorting in polarized hepatocytes occurs in the Golgi apparatus and the subapical compartment (SAC; the hepatocyte equivalent of the pericentrosomal recycling endosomes in other epithelia). In the Golgi apparatus, newly synthesized proteins and lipids destined for the apical surface are sorted into sphingolipid-cholesterol–enriched membrane microdomains (rafts). Thus, in the *trans*-Golgi network, multimembrane-spanning or polytopic apical membrane proteins are clustered in Lubrol WX-resistant membrane domains and delivered via vesicular transport directly to the apical surface (Aït Slimane *et al*., 2003). Single membrane-spanning apical proteins are segregated in other, Triton X-100–resistant membrane domains and targeted first to the basolateral surface, followed by their transport to the apical domain by transcytosis (Aït Slimane *et al*., 2003; Nyasae *et al*., 2003; Tuma and Hubbard, 2003). After surface delivery extensive membrane exchange occurs between the apical and basolateral domains, which involves endocytosis and subsequent recycling to either PM domain. The SAC plays a prominent role in the polarized delivery of proteins and lipids, and thus in maintaining cell surface polarity (Ihrke *et al*., 1998; van IJzendoorn and Hoekstra, 1999a,b; Rahner *et al*., 2000; van IJzendoorn and Mostov, 2000). Moreover, polarized membrane traffic from SAC is also important for the de novo biogenesis of apical PM domains (van IJzendoorn and Hoekstra, 2000), triggered by extracellular stimuli, including OSM (van der Wouden *et al*., 2002) and those that elicit cAMP/PKA signaling cascades (Zegers and Hoekstra, 1997). Indeed, we have previously shown that OSM activates a vesicular membrane trafficking pathway from SAC to the apical PM, which is dependent on cAMP/PKA activity (van der Wouden *et al*., 2002). Importantly, activation of this OSM-cAMP/PKA–regulated pathway is crucial for apical PM biogenesis in HepG2 cells (van der Wouden *et al*., 2002).

The pronounced effects of OSM on cell cycle progression, membrane traffic, and cell polarity prompted us to investigate the functional relationship between these events to obtain better insight into molecular mechanisms that control the establishment of apical surface domains in conjunction with cell cycle control.

MATERIALS AND METHODS

Cell Culture

HepG2 cells were grown in DMEM with 4500 mg of glucose per liter, containing 10% fetal calf serum and antibiotics. Media were changed every other day. Cells were trypsinized after reaching confluence. For experiments, cells were plated at low density onto ethanol-sterilized coverslips and analyzed 24, 48, 72, or 76 h after plating.

To synchronize cells in the G_1 phase of the cell cycle, cells were first grown in normal culture medium for 36 h to allow expansion of the cells, followed by culture in serum-free medium for 36 h. In some experiments, cells were subsequently exposed to normal culture medium containing 10% fetal calf serum (FCS) or cultured in medium supplemented with 30 μM fumonisin B1 (Sigma-Aldrich, St. Louis, MO; see *Results*), to chase the cells from G_1 into the S phase. As a control, cells were chased in serum-free medium. G_1-S-phase transition was monitored by the initiation of DNA synthesis, as evidenced by bromodeoxyuridine (BrdU) incorporation (Figures 2C and 3C). In other experiments, cells were first grown in normal culture medium for 36 h, followed by culturing in normal medium supplemented with the DNA synthesis inhibitor hydroxyurea (4 mM; Sigma-Aldrich) to synchronize the cells in S phase.

Determination of HepG2 Cell Polarity

Accurate estimation of the degree of HepG2 polarity was performed as described previously (Zegers and Hoekstra, 1997; van IJzendoorn and Hoekstra, 2000). Briefly, the cells were fixed with −20°C ethanol for 10 s, rehydrated in Hank's balanced slat solution (HBSS), and subsequently incubated with a mixture of tetramethylrhodamine B isothiocyanate-labeled phalloidin (Molecular Probes, Eugene, OR) and 5 ng/ml the nuclear stain Hoechst 33528 (Sigma-Aldrich) at room temperature for 30 min. The cells were then washed, and the number of bile canaliculi (BC; identified by the presence of dense F-actin staining around the BC) per 100 cells (identified by fluorescently labeled nuclei) was determined and expressed as the ratio [BC/100 cells]. Ten fields (each containing >50 cells) per coverslip (at least two coverslips per condition were studied) were analyzed. Cells were examined using an epifluorescence microscope (Provis AX70; Olympus, New Hyde Park, NY).

Immunostaining of HepG2 Cells

HepG2 cells were fixed in 4% paraformaldehyde (PFA) for 30 min at room temperature, washed, and permeabilized for 10 min with methanol at −20°C. After blocking with 1% bovine serum albumin (BSA) in phosphate-buffered saline (37°C; 1 h) the cells were incubated with primary antibody for 1 h at 37°C. For immunofluorescent costaining of γ-tubulin and PKA, cells were first incubated with 0.5% Triton X-100 at 4°C for 3 min, followed by fixation with ice-cold (−20°C) methanol for 5 min and blocking with 1% BSA. Monoclonal anti-p27Kip1 and anti-PKA-RIIα antibodies were bought from BD Transduction Laboratories (Lexington, KY) and used at 1:300 dilution. After incubation with the primary antibodies, cells were washed and incubated with the corresponding secondary antibody labeled with Alexa Fluor^{488} or Alexa Fluor^{594} (Molecular Probes) for 30 min at room temperature. The coverslips were mounted and analyzed by confocal microscopy (TCS SP2; Leica, Wetzlar, Germany).

BrdU Incorporation Assay

HepG2 cells were incubated with 50 mM BrdU in normal culture medium (see *Results*). Cells were then washed with HBBS and fixed with 4% PFA at room temperature for 30 min. Cells were subsequently washed with HBBS and incubated in 2 N HCl for 1 h. Cells were processed for immunofluorescence microscopy as described above. In brief, cells were incubated at 37°C for 30 min with a mouse monoclonal antibody against BrdU (1:50 dilution; Chemicon International, Temecula, CA). As secondary antibody, Alexa^{488} goat anti-mouse IgG was used (Molecular Probes). During the secondary antibody incubation, 5 ng/ml nuclear stain Hoechst 33528 was included to visualize the nuclei. The cells were then rinsed four times with HBBS, mounted, and examined by fluorescence microscopy as described above. The percentage of cells that had incorporated BrdU was quantified by determining the ratio of BrdU-positive nuclei. At least 10 fields each containing >50 cells were counted.

Analysis of p27^{Kip1} Levels by Western Blot

HepG2 cells were treated as described in *Results* and then lysed in 0.5 ml of Triton X-100 lysis buffer (10 mM triethanolamine, pH 7.4, 1.0% Triton X-100, 0.1% SDS, 100 mM NaCl, 1 mM EDTA, 1 mM EGTA, 1 mM NaF, 20 mM $Na_4P_2O_7$, and 2 mM sodium vanadate and a cocktail of protease inhibitors). Lysates were boiled for 5 min and cleared by centrifugation. Protein concentrations were determined by a bicinchoninic acid protein assay (Sigma-Aldrich), and equal amounts of proteins were separated on 10% SDS-PAGE gels, immunoblotted with monoclonal p27^{Kip1} antibodies (BD Transduction Laboratories) and detected with an enhanced chemiluminescence system (Amersham Biosciences, Piscataway, NJ). Bands representing p27^{Kip1} were quantified using Scion Image software.

Analysis of Transport of C_6-NBD-GalCer from SAC

To study the trafficking of the fluorescent GalCer analog from SAC, SAC were preloaded with the lipid as depicted in Figure 1. This procedure has been described in detail previously (van IJzendoorn and Hoekstra, 1999a, 2000). In short, cells were labeled with 4 μM C_6-NBD-GalCer at 37°C (Figure 1, step 1) to allow internalization from the basolateral surface and subsequent transcytosis to the apical BC PM domain (Figure 1, step 2). After 30 min of incubation, lipid analog still residing at the basolateral domain was depleted by a back exchange procedure at 4°C [2 × 30 min incubation in HBSS + 5% (wt/vol) BSA; Fluka, Fuchs, Switzerland; c.f. van IJzendoorn *et al*., 1997)] (Figure 1, step 3), and BC-associated lipid analog was chased into SAC at 18°C for 1 h in back exchange medium (Figure 1, step 4). Then, the NBD fluorescence at the exoplasmic BC leaflet was abolished using sodium dithionite (Merck Biosciences, Darmstadt, Germany) at 4°C, leaving the majority of the intracellular GalCer analog in SAC (Figure 1, step 5; van IJzendoorn and Hoekstra, 1998, 2000). After removal of dithionite by washing, transport from SAC was examined by incubating in back exchange medium at 37°C (Figure 1, step 6).

To quantitate transport of the lipid analog to and from the BC, the percentage of NBD-positive BC was determined as described previously (van IJzendoorn *et al*., 1997; van IJzendoorn and Hoekstra, 1998). Briefly, BC were first identified by phase contrast illumination and then categorized as NBD-positive or NBD-negative under epifluorescence illumination. Note that a BC is categorized as fluorescently labeled, i.e., NBD-positive, when microvilli-like structures, characteristic of the BC, can be detected that are seemingly fluorescent in the wake of the fluorescence derived from the lipid analog, present in the apical membrane (van IJzendoorn *et al*., 1997). Such microvilli-like structures are typically and readily observed upon gradual photobleaching of the BC-associated NBD fluorescence.

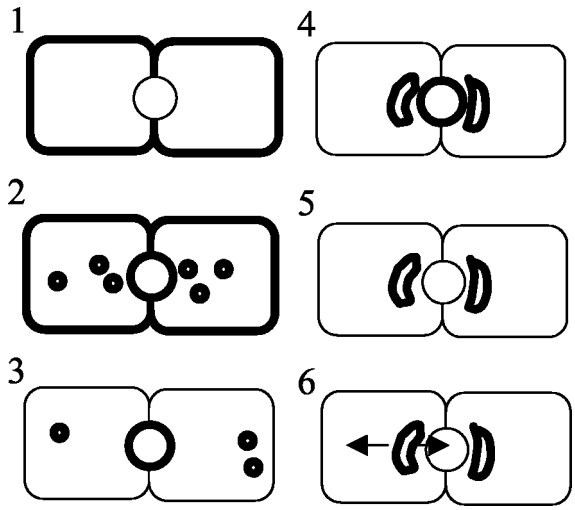

Figure 1. Schematic representation of the various steps of the lipid transport assays. The cell-labeling situation after the corresponding incubation step is depicted at the right. Cells are incubated with C_6NBD-GalCer at 37°C for 30 min, which allows incorporation of the probe in the basolateral plasma membrane (step 1) and subsequent transcytosis to the apical domain (BC; step 2). Then, the fraction of the fluorescent lipid probe still residing at the basolateral PM is depleted by BSA at 4°C twice for 30 min (step 3). The BC-associated probe is then chased into SAC at 18°C for 1 h in BSA-containing medium (step 4). The presence of BSA in the medium during this step will prevent reentry of any C_6NBD-GalCer that might arrive basolaterally during the chase. Next, the probe remaining at the BC is quenched by sodium dithionite (step 5). The sodium dithionite is removed by extensive washing with ice-cold HBSS. Occasionally, cells were subsequently incubated with OSM at 4°C for 30 min. Transport of the subapically derived fluorescent probe can be monitored upon rewarming and incubating the cells at 37°C (step 6).

Distinct pools of fluorescence are thus discerned at the apical pole of the cells, present in vesicular structures adjacent to BC, which are defined as SACs (c.f. van IJzendoorn and Hoekstra, 1998). Together, BC and SAC constitute the bile canalicular pole (BCP) in HepG2 cells (Figure 1). Therefore, within the BCP region the localization of the fluorescent lipid analog will be defined as being derived from the BC, SAC, or both. This also provides a means to describe the movement of the lipid within or out of this region in the cell (van IJzendoorn and Hoekstra, 1999a). Thus, after loading SAC with lipid analog and allowing its transport to take place as described above, the direction of movement of the lipid from or within the BCP region is determined after a given time, by establishing the distribution of the NBD-labeled lipid over the various compartments (BC, SAC, or both) that constitute the BCP, relative to the labeling (i.e., primarily SAC), before starting the chase (t = 0). For this kind of analysis, at least 50 BCP per coverslip were analyzed. Data are expressed as the mean ± SEM of at least four independent experiments, carried out in duplicate, and Student's *t* tests were carried out to determine the statistical significance of the data.

RESULTS

Cell Polarity Development Is Positively Correlated with p27^{Kip1} Expression

Well-differentiated human hepatic HepG2 cells have been successfully used for the study of membrane dynamics and polarity development in hepatocytes. Apical BC PM domains form between two adjacent cells, as readily visualized by staining the underlying actin network with fluorescently labeled phalloidin (van IJzendoorn *et al*., 1997). As shown in Figure 2A, HepG2 cells acquire PM polarity in time, as evidenced by the ratio BC/100 cells, and reach optimal polarity 3 d after plating (Figure 2A; c.f. van IJzendoorn and Hoekstra, 2000). Treatment of the cells with dibutyryl (db) cAMP or the interleukin-6 family cytokine oncostatin M stimulates polarity development, i.e., apical PM biogenesis in HepG2 cells (Figure 2A, black bars and gray bars, respectively, c.f. van der Wouden *et al*., 2002), as evidenced by a 2.4- and 1.5-fold increase in the ratio BC/100 cells at 24 and 48–72 h, respectively, after plating. Similar results were obtained with other stable cAMP analogs, and the adenylate

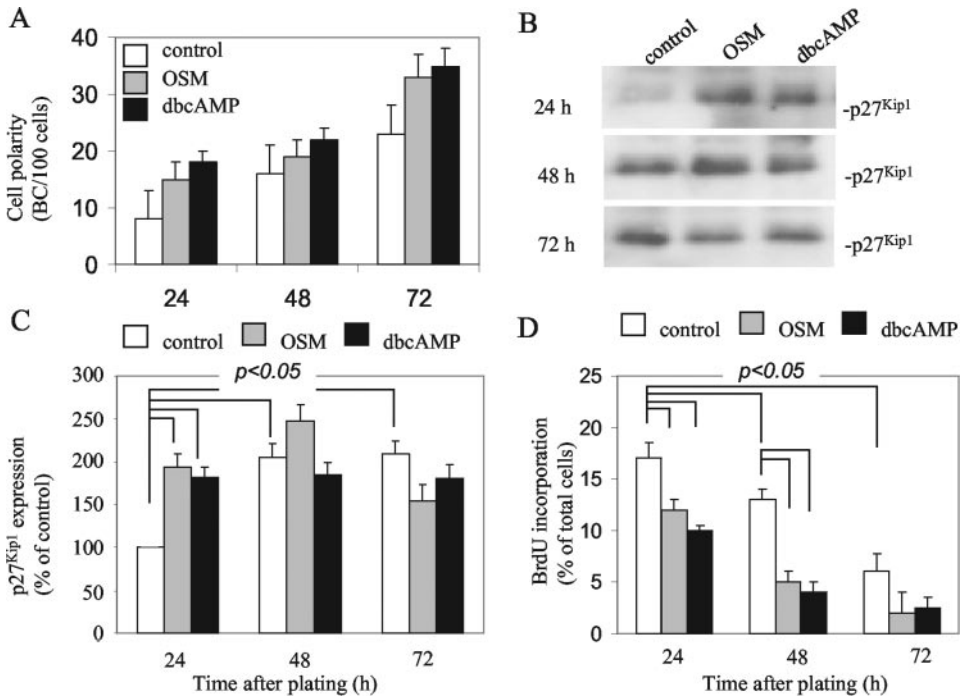

Figure 2. Cell polarity development is positively correlated to p27^{Kip1} expression and G_1 phase arrest. (A) The ratio BC/100 cells was determined at different times in cells cultured on coverslips in normal culture medium (white bars) or normal culture medium supplemented with OSM (gray bars) or dbcAMP (black bars). (B) Cells were cultured in medium supplemented or not with OSM or dbcAMP for different times. Cells were then lysed, and p27^{Kip1} expression was examined by Western blot. A representative blot of three independent experiments is shown. (C) Expression levels of p27Kip1 (as depicted in B) were quantified using Scion Image software. The percentage of increase compared with nontreated cells (set to 100%) of three independent experiments is shown ($p < 0.05$ in Student's *t* test). (D) Cells were cultured in black bars) for different times. Twenty-four hours before analysis, BrdU was included in the culture medium. Cells were fixed and stained with anti-BrdU antibodies and the DNA stain Hoechst for immunofluorescence analysis. Note the decreased incorporation of BrdU in OSM- and dbcAMP-treated cells compared with control cells ($p < 0.05$ in Student'a *t* test), indicative for inhibited G_1-S-phase transition.

cyclase agonist forskolin, but not with sodium butyrate (data not shown; c.f. Zegers and Hoekstra, 1997).

Although the process of cell differentiation generally seems negatively correlated with cellular proliferation, it is not clear whether cell polarity and proliferation are directly, e.g., genetically, linked or that one is an indirect by-effect of the other. We observed that after plating, the expression of $p27^{Kip1}$ increases significantly (approximately twofold) during the first 48 h, after which it remains at a constant level (Figure 2, B and C, white bars). $p27^{Kip1}$ plays a critical role in mediating cell cycle exit by inhibiting the activity of cyclinE/cdk2, a kinase that is required for the transition of cells from the G_1 phase, i.e., the gap between mitosis and the next round of DNA synthesis, into S phase. In agreement with the observed increase in $p27^{Kip1}$ expression, the number of cells that enter S phase and start DNA synthesis is reduced, as evidenced by a decreased incorporation of the thymidine analog BrdU (Figure 2D). Treatment of the cells with oncostatin M (10 ng/ml) enhances the increase in $p27^{Kip1}$ expression during the first 48 h (Figure 2, B and C, gray bars) and results in a more pronounced arrest in the G_1 phase (Figure 2D, gray bars). Similar results were obtained with dibutyryl cAMP (Figure 2, B–D, black bars), well-known to stimulate cell polarity development (Figure 2A, black bars; c.f. Zegers *et al*., 1997; van IJzendoorn and Hoekstra, 1999, 2000), and after serum deprivation (Figure 3). Together, oncostatin M- and cAMP-stimulated cell polarity, i.e., apical PM biogenesis, is positively correlated with $p27^{Kip1}$ expression and G_1-phase arrest.

Down-Regulation of $p27^{Kip1}$ Expression and Subsequent S-Phase Entry Inhibits Oncostatin M-stimulated Polarity Development

We next investigated whether control of G_1-S-phase progression by $p27^{Kip1}$ is functionally coupled to apical PM biogenesis. To this end, cells were cultured for 36 h in normal cell culture medium to allow expansion of the cells, followed by serum deprivation for another 36 h to synchronize the cells in the G_1 phase. Cells were then stimulated with medium supplemented with (SS) or without (SD) 10% FCS and oncostatin M, in the presence of BrdU for 4 h (Figure 3A). In parallel, cells were grown in normal culture medium for 76 h without medium refreshment for comparison (control; C). As shown in Figure 3, B and C, serum deprivation resulted in increased levels of $p27^{Kip1}$ (~1.4-fold), whereas the subsequent stimulation with serum, but not buffer, resulted in the marked down-regulation of $p27^{Kip1}$ expression (~40%). In agreement with this, few cells entered S phase in serum-deprived cells, whereas, by contrast, ~70% of the cells (~3.5-fold increase) entered S phase after serum stimulation, as evidenced by a massive BrdU incorporation (Figure 3D). The mitotic index in serum-stimulated cell cultures was <3% (unpublished data). Importantly, whereas oncostatin M effectively stimulated cell polarity development in serum-deprived cells by ~45%, as evidenced by an increased ratio of apical PM domains per number of cells, serum-stimulated cells were found to be completely insensitive to oncostatin M stimulation with respect to apical PM biogenesis (Figure 3E).

Similar effects were observed with hydroxyurea ($CH_4N_2O_2$). Hydroxyurea inactivates ribonucleoside reductase, thereby blocking deoxynucleotide synthesis and arresting the cells in S phase (Balczon *et al*., 1995; Khodjakov *et al*., 2002). HepG2 cells were cultured for 36 h in normal culture medium to allow expansion of the cells and then treated with 4 mM hydroxyurea for 36 h, followed by incubation in medium containing OSM and hydroxyurea for 4 h (Figure 4A). Hydroxyurea prevented DNA synthesis in HepG2 cells as evidenced by reduced BrdU incorporation compared with nontreated cells (73% reduction; c.f. Chouteau *et al*., 2001). As shown in Figure 4B, hydroxyurea rendered the cells insensitive to the polarity-stimulating effects of OSM very similar as observed in serum-stimulated cells (c.f. Figure 3D).

As an alternative approach to drive cells from G_1 into the S phase, the cells were treated with the mycotoxin fumonisin B1 (FB1) which, in HepG2 cells, results in a decrease in $p27^{Kip1}$ expression of ~75% (Figure 5A). As a consequence, cells treated with FB1 shifted from the G_1 to S phase, evidenced by an increase in the number of cells that had incorporated BrdU (Figure 5A, inset). Treatment of the cells with FB1 inhibits polarity development (Figure 5B). We then examined the effect of FB1-mediated down-regulation of $p27^{Kip1}$ expression on the ability of oncostatin M to stimulate apical PM biogenesis. Oncostatin M failed to stimulate polarity development in FB1-treated cells (Figure 5B), similarly as observed in serum-stimulated or hydroxyurea-treated cells (Figures 3D and 4).

Down-regulation of $p27^{Kip1}$ expression and subsequent G_1-S-phase transition is typically mediated by the increased activity of cyclin-dependent kinase (cdk)2. Indeed, when serum-deprived cells were incubated with the cdk2 inhibitor roscovitin during subsequent serum or FB1 stimulation, cells failed to enter S phase, as evidenced by a lack of increased BrdU incorporation (unpublished data). Importantly, cdk2-inhibited cells retained their sensitivity to the polarity-stimulating effects of oncostatin M after serum or FB1 stimulation (Figure 5B). These data thus suggest that $p27^{Kip1}$ down-regulation by itself is not sufficient but requires cdk2 activity to render the cells insensitive to the polarity-stimulating effects of oncostatin M. Conversely, the down-regulation of cdk2 activity, mediated by OSM-stimulated $p27^{Kip1}$ expression, thus seems an important parameter in OSM-stimulated apical PM biogenesis.

G_1-S Phase Transition Pertubs Oncostatin M-regulated Polarized Membrane Trafficking

In hepatocytes, the SAC, the equivalent of the common endosome in other epithelial cells (van IJzendoorn and Hoekstra, 1999b; van IJzendoorn *et al*., 2000) plays a crucial role in polarity development. In previous studies, we have demonstrated that polarity development in HepG2 cells requires the activation of a vesicular trafficking route exiting SAC and directed toward the developing BC, which can be monitored by the flow of the fluorescent probes C_6-NBD-SM and C_6-NBD-GalCer (van IJzendoorn and Hoekstra, 1999a,b, 2000). Oncostatin M activates this pathway to stimulate apical PM biogenesis (van der Wouden *et al*., 2002). The question thus arises whether up-regulation of $p27^{Kip1}$ expression and, consequently, inhibition of G_1-S-phase transition, is required for oncostatin M to exert its effects on membrane traffic. To investigate this, cells were synchronized using serum deprivation/stimulation, according to the incubation scheme depicted in Figure 3A, and SAC was preloaded with C_6-NBD-GalCer as described in detail in *Materials and Methods* (c.f. van der Wouden *et al*., 2002). A scheme depicting the incubation steps is shown in Figure 1. Note that the trafficking steps necessary for loading SAC, i.e., basolateral endocytosis, apical delivery and apical PM-to-SAC transport, were not visibly affected by the synchronization procedure (Figure 6, A and D). After loading of the fluorescent lipid analogue in SAC, cells were treated with oncostatin M or medium at 4°C (Figure 1, step 5), warmed to 37°C, and lipid flow from SAC to either apical (BC) or basolateral membrane was followed for 20 min in serum-free medium or normal

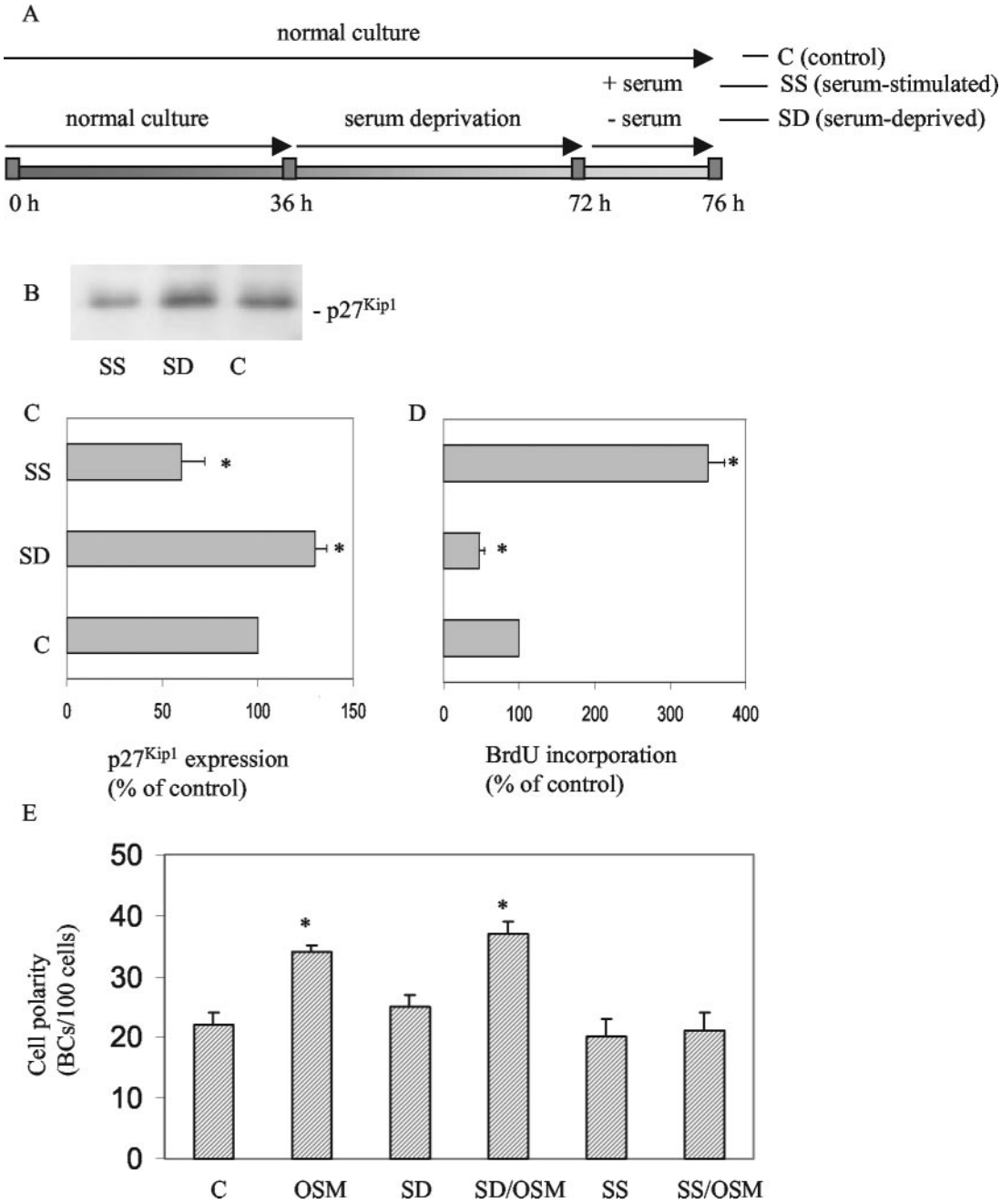

Figure 3. Effect of OSM on polarity development in G_1- and S-phase HepG2 cells. (A) Scheme depicting how cells are synchronized and treated with OSM in the G_1 and S phase of the cell cycle. (B) Expression levels of $p27^{Kip1}$ in serum-deprived (SD), serum-stimulated (SS), and control (C) cells. (C) Quantification of the relative expression levels of $p27^{Kip1}$ in SD, SS compared with C cells. (D) Relative changes in the incorporation of BrdU in SD, SS compared with C cells. (E) Effect of OSM on polarity development in SD, SS, and C cells.

culture medium (Figure 1, step 6). In control (i.e., serum-deprived; G_1) cells, C_6-NBD-GalCer disappeared during this time interval from the BCP, which comprises SAC (where the lipid is located at t = 0; Figure 6A) and BC. Indeed, the percentage of BCP that contained C_6-NBD-GalCer decreased in time (Table 1). The relative distribution of the lipid analogue in the remaining, faintly labeled C_6-NBD-GalCer-positive BCP shows that the probe predominantly resided in SAC and little, if any, movement from SAC to BC could be detected (Table 1; Figure 6B, compare with 6A). Rather, these data indicate that the probe was transported from SAC to the basolateral domain of the cells, consistent with previous observations (van IJzendoorn and Hoekstra, 1999a, 2000). By contrast, in oncostatin M-treated G_1 cells, C_6-NBD-GalCer remained associated with the BCP region during the 20-min chase, as evidenced by the unchanged percentage of BCP that contained C_6-NBD-GalCer (Table 1). Analysis of the corresponding relative distribution of the probe in the BCP reveals a flow of the lipid analogue from SAC to BC (Table 1; Figure 6C, compare to 6B; cf. van IJzendoorn and Hoekstra, 1999a, 2000). In striking contrast, oncostatin M failed to target C_6-NBD-GalCer from SAC to BC in serum-

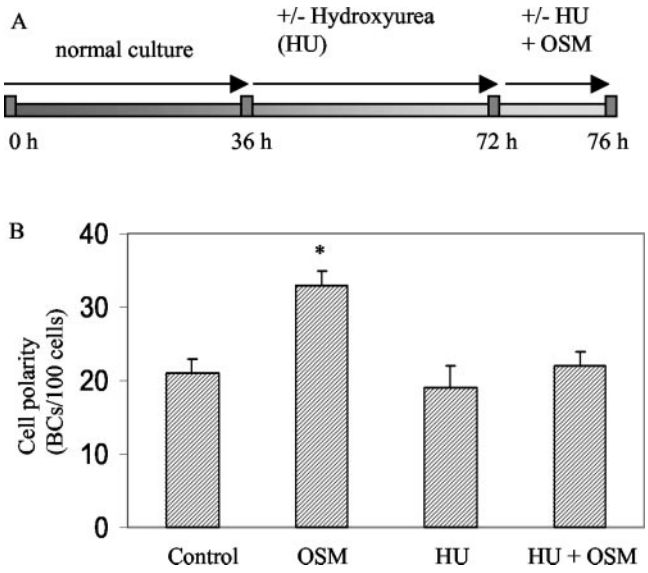

Figure 4. Effect of hydroxyurea (HU) on OSM-stimulated polarity development. (A) Scheme depicting how cells are synchronized with HU (4 mM). (B) HU inhibits the cell polarity-stimulating effects of OSM.

stimulated cells, i.e., cells that had entered S phase (Table 1; Figure 6F, compare with 6E). Thus, in serum-stimulated cells, C_6-NBD-GalCer remained associated with the BCP during the 20-min chase (Table 1), and analysis of the relative distribution of the lipid analogue in the labeled BCP revealed that most C_6-NBD-GalCer localized to SAC (Table 1; Figure 6F), indicating entrapment of the lipid in SAC. Serum stimulation did not affect transport of the fluorescent lipid exiting SAC in the basolateral direction (Figure 6, E vs. B). These data strongly suggest that a minimal level of $p27^{Kip1}$ expression, sufficient for G_1 arrest, is a prerequisite for oncostatin M signaling to specifically activate SAC-to-BC trafficking route and, in this way, to stimulate polarity development.

Treatment of the cells with the cdk2 inhibitor roscovitin shortly before and during serum stimulation, thereby precluding G_1-S phase transition, rescued the ability of OSM to activate SAC-to-BC route followed by C_6-NBD-GalCer (Table 1; Figure 6G, compare with 6C and 6F) and, presumably in this way, apical PM biogenesis (Figure 5), implicating the involvement of cdk2 activity.

G_1-S-Phase Transition Inhibits OSM-stimulated Recruitment of PKA to the Centrosomal Region

The ability of OSM to activate SAC-to-apical surface route requires cAMP/PKA activity, as evidenced by using pharmacological inhibitors of PKA (van der Wouden *et al*., 2002). Although OSM did not give rise to increased cAMP or PKA expression levels, a significant recruitment of PKA to the centrosome region was noted (van der Wouden *et al*., 2002). To determine whether the OSM-stimulated recruitment of PKA to the centrosome region corresponds to its ability to activate the SAC-to-BC pathway, we examined the effect of G_1-S-phase transition on the ability of OSM to stimulate centrosomal PKA recruitment. For this, cells were synchronized in G_1 by serum deprivation and subsequently incubated for 4 h in serum-free medium (which maintains the cells in G_1) or in FCS-containing medium (which drives the cells into the S-phase), both supplemented with OSM. Cells were then fixed and stained with antibodies raised against the centrosomal protein γ-tubulin and PKA. The percentage of PKA-positive centrosomes (identified by γ-tubulin) was then determined. As shown in Table 2, OSM stimulated the recruitment of PKA to centrosome region in G_1 cells (~24% more γ-tubulin–labeled centrosomes were positive for PKA). Illustrative immunofluorescence pictures are shown in Figure 7, A–F. In striking contrast, OSM failed to recruit PKA to the centrosome region in S-phase cells (Table 2). In fact, 13% less γ-tubulin–labeled centrosomes in serum-stimulated cells displayed PKA association, and OSM failed to stimulate PKA recruitment at the centrosomal region (Table 2 and Figure 7, G–L). In serum-stimulated cells, but not in serum-deprived cells, some PKA localized to the nucleus. Given that PKA is required for OSM to activate the SAC-to-BC transport pathway and apical PM biogenesis, the apparent inability of OSM to recruit PKA to the centrosome region upon G_1-S-phase transition possibly is part of the underlying mechanism responsible for rendering the cells insensitive to OSM with regard to apical PM biogenesis.

DISCUSSION

In this study, we have addressed the functional relationship between cell cycle regulation and the acquisition of a polarized phenotype, i.e., apical PM biogenesis, in hepatic HepG2 cells in response to OSM signaling. First, we demonstrate that (OSM-stimulated) apical PM biogenesis in HepG2 cells displays a strong positive correlation with expression levels of the cell cycle regulatory protein $p27^{Kip1}$ and subsequent G_1-phase arrest. Indeed, exposure of the cells to OSM en-

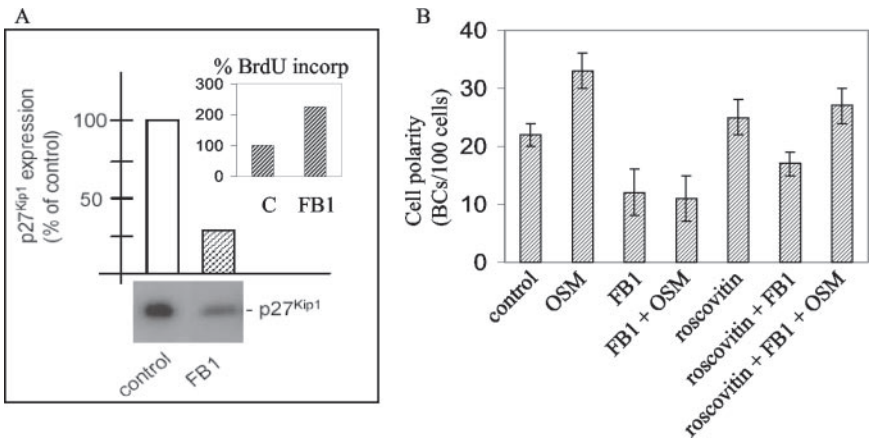

Figure 5. Effect of FB1 on cell cycle and OSM-mediated polarity development. (A) FB1 down-regulates $p27^{Kip1}$ expression (blot and quantification) and promotes S-phase entry, as evidenced by BrdU incorporation (inset). (B) FB1 inhibits OSM-stimulated polarity development in HepG2 cells. Note that the cdk2 inhibitor roscovitin restores the stimulatory effect of OSM on polarity development in FB1-treated cells.

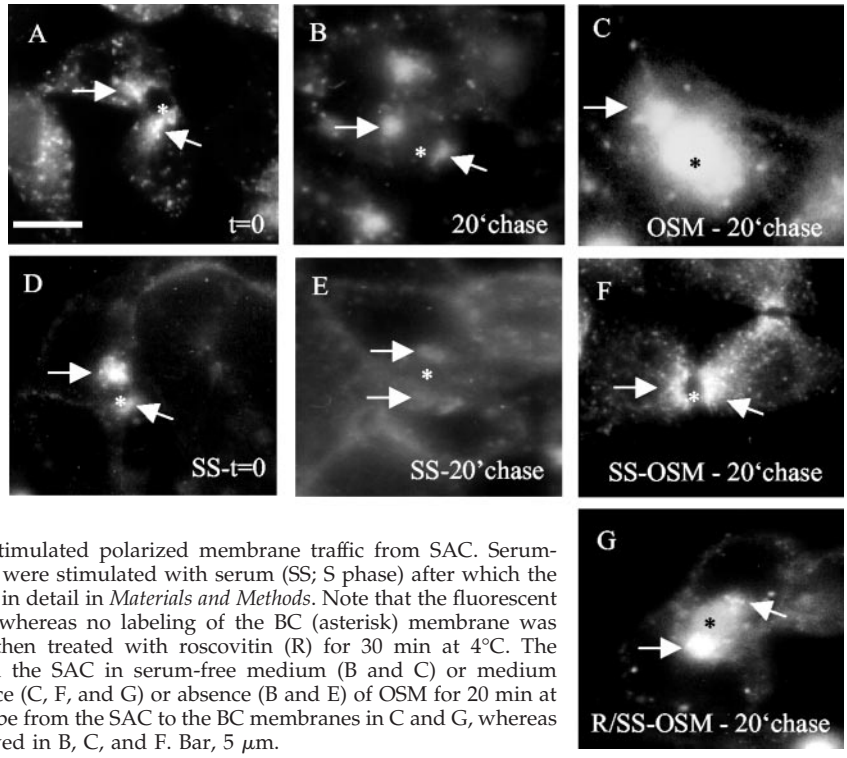

Figure 6. G_1-S-phase transition perturbs OSM-stimulated polarized membrane traffic from SAC. Serum-deprived cells kept in serum-free medium (G_1) or were stimulated with serum (SS; S phase) after which the SAC was loaded with C_6NBD-GalCer as described in detail in *Materials and Methods*. Note that the fluorescent probe predominantly labeled the SAC (arrows), whereas no labeling of the BC (asterisk) membrane was observed. In some experiments (G), cells were then treated with roscovitin (R) for 30 min at 4°C. The fluorescent probe was subsequently chased from the SAC in serum-free medium (B and C) or medium supplemented with serum (SS, E–G) in the presence (C, F, and G) or absence (B and E) of OSM for 20 min at 37°C. Note the redistribution of the fluorescent probe from the SAC to the BC membranes in C and G, whereas no redistribution from SAC to BC could be observed in B, C, and F. Bar, 5 μm.

hances the expression of $p27^{Kip1}$ and prevents entry of the cells in S phase as evidenced by the inhibition of BrdU incorporation (Figure 2). This is in agreement with the findings of Klausen *et al.* (2000), which showed that OSM inhibits cell cycle progression by preventing $p27^{Kip1}$ degradation in HepG2 cells. Importantly, our data indicate that apical PM biogenesis stimulated by OSM is critically dependent on the ability of OSM to control $p27^{Kip1}$/cdk2-mediated G_1-S-phase progression. Thus, asynchronous cells readily respond to OSM signaling with regard to apical PM biogenesis, and serum deprivation, which results in increased $p27^{Kip1}$ expression and synchronization of the cells in G_1-phase, enhances the stimulatory effect of OSM (Figure 3). In striking contrast, serum- or FB1-stimulated down-regulation of $p27^{Kip1}$ expression levels, allowing G_1-S-phase transition to occur, effectively renders the cells insensitive to the cell polarity-stimulating effects of OSM (Figures 2 and 3). Indeed, cells similarly acquire insensitivity to the polarity-stimulating effects of OSM after hydroxyurea-induced S-phase arrest (Figure 4). $p27^{Kip1}$ down-regulation results in an expected net increase in cdk2 activity, which plays an important role in G_1-S-phase transition (Ekholm and Reed, 2000; Woo and Poon, 2003). Inhibition of cdk2 activity in HepG2 cells with roscovitin prevented G_1-S-phase transition and kept the cells responsive to the polarity-stimulating effects of OSM, even in the serum- or FB1-treated cells. Together, our data indicate that extracellular signal- and $p27^{Kip1}$/cdk2-regulated cell cycle progression controls de novo apicalization of the cell surface.

Serum-stimulated G_1-S-phase transition effectively inhibits the OSM-stimulated and PKA-dependent activation of a membrane transport pathway exiting the SAC and directed toward the developing apical surface (Table 1 and Figure 6). The activation of this membrane trafficking pathway has previously been demonstrated to play an important role in apical-basolateral polarity development in HepG2 cells (van IJzendoorn and Hoekstra, 1999a,b; van IJzendoorn *et al.*, 2000; Hoekstra *et al.*, 2004). OSM-stimulated membrane trafficking from SAC to the developing apical surface is dependent on intact microtubules (unpublished data). Serum-stimulated G_1-S-phase transition, however, did not visibly affect the spatial organization of SAC (Figure 6) and also the distribution of the microtubule cytoskeleton was not visibly altered (unpublished data), supporting the notion that se-

Table 1. G_1-S-phase transition perturbs OSM-stimulated polarized membrane traffic from SAC

	0-min chase	20-min chase G_1-control	20-min chase G_1-OSM	20-min chase SS-OSM	20-min chase R/SS-OSM
% Positive BCP	89 (2)	63 (4)*	88 (3)	90 (2)	84 (4)
Relative distribution in BCP					
SAC	84 (3)	79 (3)	40 (2)*	89 (3)	30 (4)*
BC + SAC	17 (2)	21 (3)	30 (4)*	11 (2)	20 (1)
BC	3 (1)	2 (1)	35 (3)*	3 (1)	45 (3)*

* $p < 0.05$.

Table 2. Effect of serum-stimulated G_1-S-phase transition on OSM-stimulated recruitment of PKA to the centrosomal region

	% Increase in PKA-positive centromes
Control	0
OSM	+24 ± 4*
SS-control	−13 ± 4*
SS-OSM	−12 ± 3*

* $p < 0.01$ (OSM vs. control; SS-control vs. control; SS-OSM vs. OSM).

SS, serum starved.

rum-stimulated cells had not reached prophase during which microtubules are rearranged to form spindles, and indicating that the observed S-phase entry-induced impairment of OSM-regulated polarized membrane traffic from SAC is not likely the result of a cell cycle-related reorganization of the microtubule cytoskeleton.

The OSM-stimulated and PKA-dependent reorganization of polarized membrane trafficking from SAC coincides with a stimulated recruitment of PKA to the centrosomal region (van der Wouden *et al*., 2002). The SAC and other organelles involved in polarized sorting, e.g., the Golgi apparatus, are typically concentrated in the centrosomal region (Hobdy-Henderson *et al*., 2003; Rios and Bornens, 2003), and both the centrosome and associated organelles typically face specialized cell surface domains, e.g., the leading lamella in migrating fibroblasts (Ueda *et al*., 1997) and the apical PM domain in epithelial cells (Buendia *et al*., 1990). Moreover, in differentiated G_1 cells, one of the centrosomes moves to the apical surface to form the basal body of the primary cilium, a highly specialized membrane domain that extends from the apical surface. The functional relevance for the clustering of SAC and Golgi around the centrosome is not clear, but it may serve a purpose in integrating complex signaling cascades (Lange, 2002; Rios and Bornens, 2003). In addition, recent evidence suggests that the centrosome positions organelles in proximity to specific target membranes. This may then facilitate or reinforce cytoskeleton remodeling and/or membrane exchange between organelles and the cell surface necessary for the biogenesis of specialized PM domains, such as the apical surface (Wald *et al*., 2003) or the furrow during cytokinesis (Riggs *et al*., 2003). Serum-triggered G_1-S-phase transition effectively inhibits the OSM-stimulated recruitment of PKA to the centrosomal region (Table 2 and Figure 7). This is in agreement with the finding that the displacement of PKA from centrosomes positively modulates G_1-S-phase transition (Feliciello *et al*., 2000). Interestingly, very similar to the observed inhibition of de novo polarity development upon G_1-S-phase transition (Figures 3 and 4), the stimulatory effect of OSM on apical PM biogenesis in HepG2 cells is abolished when cAMP/PKA activity is inhibited (van der Wouden *et al*., 2002). These data suggest that recruitment of PKA to the centrosomal region is required for OSM to activate a membrane traffic route from SAC to the developing apical surface, and in this way, stimulate apical PM biogenesis. This underscores the importance of the centrosomal region as a specialized site where complex cellular events, including cell cycle progression and membrane traffic, are coordinately integrated (Rieder *et al*.,

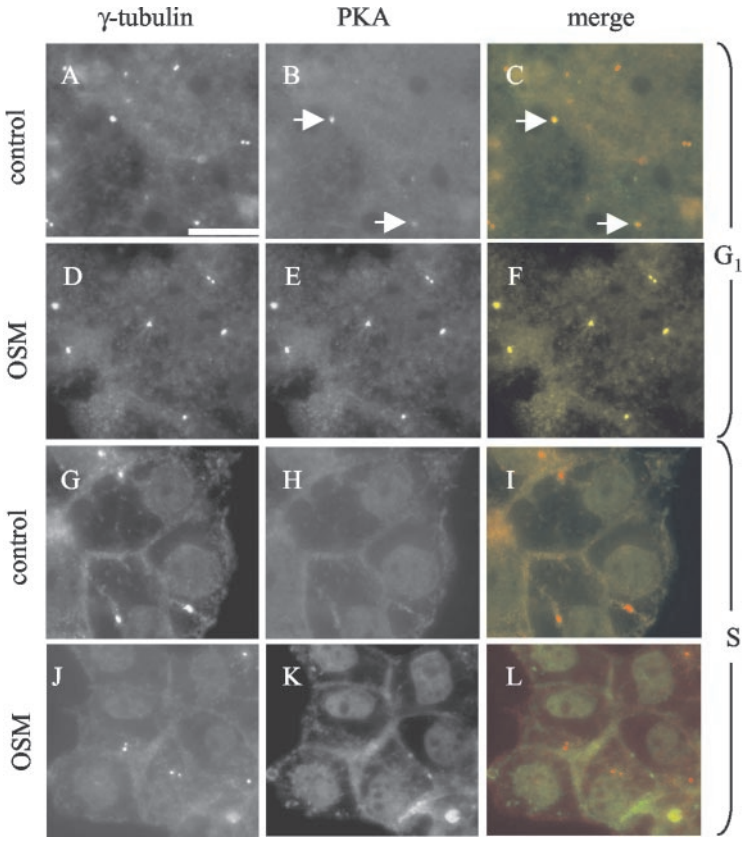

Figure 7. Effect of serum-stimulated G_1-S-phase transition on OSM-stimulated recruitment of PKA to the centrosomal region. Serum-deprived cells were kept in serum-free medium (to keep them in G_1; A–F) or were stimulated with serum (to drive them in the S phase; G–L) in the presence (D–F, J–L) or absence (A–C, G–I) of OSM. The cells were then fixed and labeled with antibodies against γ-tubulin and PKA as described in *Materials and Methods*. The percentage of γ-tubulin–positive centrosomes that were labeled with PKA was determined and representative pictures were taken. Note that OSM stimulates the recruitment of PKA to γ-tubulin–positive centrosomes (dotted appearance) in G_1 cells (compare D–F with A–C) but not in S-phase cells (compare J–L with G–I). Arrows in B and C point to centrosomes positive for both γ-tubulin and PKA. In D–F, all γ-tubulin–positive centrosomes shown are also positive for PKA. C, F, I, and L show merged images with γ-tubulin in red and PKA in green. Bars, 10 μm.

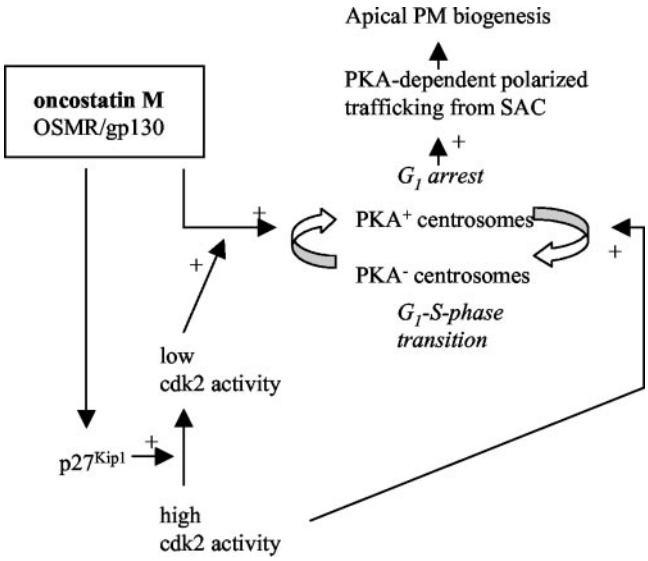

Figure 8. Working model. A detailed explanation is provided in *Discussion*.

2001), and it implicates OSM as an important regulating factor in this. At present, a molecular link between cdk2 activity at the G_1/S-boundary and PKA association at the centrosome is unclear. However, such a link is not unprecedented because mitotic CDK1 activity has been demonstrated to displace PKA from centrosomal A-kinase anchoring proteins. We are currently investigating the molecular mechanism by which OSM stimulates PKA recruitment to the centrosomal region and the identification of OSM-controlled PKA targets.

Based on the data, we propose a model (Figure 8) in which OSM signaling enhances $p27^{Kip1}$ expression, and consequently down-regulates cdk2 activity, resulting in G_1 arrest. Low cdk2 activity allows OSM-stimulated recruitment of PKA to the centrosomal region that is essential for mediating the OSM-activated membrane exchanges between SAC and the developing apical surface. On G_1-S-phase transition, induced by circulating growth factors or mitogenic mycotoxins such as FB1 (Schroeder *et al*., 1994; this study), the increasing cdk2 activity may not be sufficiently down-regulated by OSM and therefore interferes with OSM-mediated recruitment of PKA to the centrosomal region. This then impairs the regulated membrane supply from the pericentrosomal SAC to the cell surface and hence apical PM biogenesis. This model underscores the recently suggested role of endosomal recycling in the spatial-temporal control of plasma membrane insertion that is required for cell morphogenesis (Lecuit, 2003; Pelissier *et al*., 2003), e.g., the development of the apical domain, and it places PKA-regulated polarized plasma membrane recycling under control of $p27^{Kip1}$/cdk2-regulated G_1-S-phase transition.

ACKNOWLEDGMENTS

We thank Karin Klappe for help with the synthesis of C_6-NBD–labeled sphingolipids. S.C.D.v.I. was supported by the Royal Dutch Academy of Sciences (KNAW).

REFERENCES

Aït Slimane, T.A., Trugnan, G., van IJzendoorn, S.C., and Hoekstra, D. (2003). Raft-mediated trafficking of apical resident proteins occurs in both direct and transcytotic pathways in polarized hepatic cells: role of distinct lipid microdomains. Mol. Biol. Cell *14*, 611–624.

Albertson, R., and Doe, C.Q. (2003). Dlg, Scrib and Lgl regulate neuroblast cell size and mitotic spindle asymmetry. Nat. Cell Biol. *5*, 166–170.

Baas, A., Kuipers, J., van der Wel, N., Batlle, E., Koerten, H., Peter, P.J., and Clevers, H.C. (2004). Complete polarization of single intestinal epithelial cells upon activation of LKB1 by STRAD. Cell *116*, 457–466.

Balczon, R., Bao, L., Zimmer, W.E., Brown, K., Zinkowski, R.P., and Brinkley, B.R. (1995). Dissociation of centrosome replication events from cycles of DNA synthesis and mitotic division in hydroxyurea-arrested Chinese hamster ovary cells. J. Cell Biol. *130*, 105–115.

Bilder, D., Li, M., and Perrimon, N. (2000). Cooperative regulation of cell polarity and growth by *Drosophila* tumor suppressors. Science *289*, 113–116.

Buendia, B., Bre, M.H., Griffiths, G., and Karsenti, E. (1990). Cytoskeletal control of centrioles movement during the establishment of polarity in Madin-Darby canine kidney cells. J. Cell Biol. *110*, 1123–1135.

Chagraoui, J., Lepage-Noll, A., Anjo, A., Uzan, G., and Charbord, P. (2003). Fetal liver stroma consists of cells in epithelial-to-mesenchymal transition. Blood. *101*, 2973–2982.

Chouteau, P., Le Seyec, J., Saulier-Le Drean, B., Cannie, I., Brissot, P., Lescoat, G., Guguen-Guillouzo, C., and Gripon, P. (2001). Inhibition of hepatitis B virus production associated with high levels of intracellular viral DNA intermediates in iron-depleted HepG2.2.15 cells. J. Hepatol. *34*, 108–113.

Ekholm, S.V., and Reed, S.I. (2000). Regulation of G(1) cyclin-dependent kinases in the mammalian cell cycle. Curr. Opin. Cell Biol. *12*, 676–684.

Feliciello, A., Gallo, A. Mele, E., Porcellini, A., Troncone, G., Garbi, C., Gottesman, M.E., Avvedimento, E.V. (2000). The localization and activity of cAMP-dependent protein kinase affect cell cycle progression in thyroid cells. J. Biol. Chem. *275*, 303–311.

Hanada, S., Kayano, H., Jiang, J., Kojima, N., Miyajima, A., Sakoda, A., and Sakai, Y. (2003). Enhanced in vitro maturation of subcultivated fetal human hepatocytes in three dimensional culture using poly-L-lactic acid scaffolds in the presence of oncostatin M. Int. J. Artif. Organs *26*, 943–951.

Hoekstra, D., Tyteca, D., and van IJzendoorn, S.C.D. (2004). The subapical compartment: a traffic center in membrane polarity development. J. Cell Sci. *117*, 2183–2192.

Hobdy-Henderson, K.C., Hales, C.M., Lapierre, L.A., Cheney, R.E., and Goldenring, J.R. (2003). Dynamics of the apical plasma membrane recycling system during cell division. Traffic *4*, 681–693.

Hui, A.M., Makuuchi, M., and Li, X. (1998). Cell cycle regulators and human hepatocarcinogenesis. Hepatogastroenterology *45*, 1635–1642.

Humbert, P., Russell, S., and Richardson, H. (2003). Dlg, Scribble and Lgl in cell polarity, cell proliferation and cancer. Bioessays *25*, 542–553.

Ihrke, G., Martin, G.V., Shanks, M.R., Schrader, M., Schroer, T.A., and Hubbard, A.L. (1998). Apical plasma membrane proteins and endolyn-78 travel through a subapical compartment in polarized WIF-B hepatocytes. J. Cell Biol. *141*, 115–133.

Kamiya, A., Inoue, Y., and Gonzalez, F.J. (2003). Role of the hepatocyte nuclear factor 4alpha in control of the pregnane X receptor during fetal liver development. Hepatology *37*, 1375–1384.

Kamiya, A., *et al*. (1999). Fetal liver development requires a paracrine action of oncostatin M through the gp130 signal transducer. EMBO J. *18*, 2127–2136.

Kamiya, A., Kinoshita, T., and Miyajima, A. (2001). Oncostatin M and hepatocyte growth factor induce hepatic maturation via distinct signaling pathways. FEBS Lett. *492*, 90–94.

Kamiya, A., Kojima, N., Kinoshita, T., Sakai, Y., and Miyaijma, A. (2002). Maturation of fetal hepatocytes in vitro by extracellular matrices and oncostatin M: induction of tryptophan oxygenase. Hepatology *35*, 1351–1359.

Khodjakov, A., Rieder, C.L., Sluder, G., Cassels, G., Sibon, O., and Wang, C.L. (2002). De novo formation of centrosomes in vertebrate cells arrested during S phase. J. Cell Biol. *158*, 1171–1181.

Kinoshita, T., and Miyajima, A. (2002). Cytokine regulation of liver development. Biochim. Biophys. Acta *1592*, 303–312.

Klausen, P., Pedersen, L., Jurlander, J., and Baumann, H. (2000). Oncostatin M and interleukin 6 inhibit cell cycle progression by prevention of p27kip1 degradation in HepG2 cells. Oncogene *19*, 3675–3683.

Klezovitch, O., Fernandez, T.E., Tapscott, S.J., and Vasioukhin, V. (2004). Loss of cell polarity causes severe brain dysplasia in Lgl1 knockout mice. Genes Dev. *18*, 559–571.

Kojima, N., Kinoshita, T., Kamiya, A., Nakamura, K., Nakashima, K., Taga, T., and Miyajima, A. (2000). Cell density-dependent regulation of hepatic devel-

opment by a gp130-independent pathway. Biochem. Biophys. Res. Commun. *277*, 152–158.

Kortylewski, M., Heinrich, P.C., Mackiewicz, A., Schniertshauer, U., Klingmuller, U., Nakajima, K., Hirano, T., Horn, F., and Behrmann, I. (1999). Interleukin-6 and oncostatin M-induced growth inhibition of human A375 melanoma cells is S.T.A.T-dependent and involves upregulation of the cyclin-dependent kinase inhibitor p27/Kip1. Oncogene *18*, 3742–3753.

Lange, B.M. (2002). Integration of the centrosome in cell cycle control, stress response and signal transduction pathways. Curr. Opin. Cell Biol. *14*, 35–43.

Lazaro, C.A., Croager, E.J., Mitchell, C., Campbell, J.S., Yu, C., Foraker, J., Rhim, J.A., Yeoh, G.C., and Fausto, N. (2003). Establishment, characterization, and long-term maintenance of cultures of human fetal hepatocytes. Hepatology *38*, 1095–1106.

Lecuit, T. (2003). Regulation of membrane dynamics in developing epithelia. Curr. Opin. Genet. Dev. *13*, 351–357.

Lecuit, T., and Pilot, F. (2003). Developmental control of cell morphogenesis: a focus on membrane growth. Nat. Cell Biol. *5*, 103–108.

Li, C., Ahlborn, T.E., Kraemer, F.B., and Liu, J. (2001). Oncostatin M-induced growth inhibition and morphological changes of MDA-MB231 breast cancer cells are abolished by blocking the MEK/ERK signaling pathway. Breast Cancer Res. Treat. *66*, 111–121.

Liu, H., Radisky, D.C., Wang, F., and Bissell, M.J. (2004). Polarity and proliferation are controlled by distinct signaling pathways downstream of PI3-kinase in breast epithelial tumor cells. J. Cell Biol. *164*, 603–612.

Matsui, T., Kinoshita, T., Morikawa, Y., Tohya, K., Katsuki, M., Ito, Y., Kamiya, A., and Miyajima, A. (2002). K-Ras mediates cytokine-induced formation of E-cadherin-based adherens junctions during liver development. EMBO J. *21*, 1021–1030.

Mostov, K., Su, T., ter Beest, M. (2003). Polarized epithelial membrane traffic: conservation and plasticity. Nat. Cell Biol. *5*, 287–293.

Nyasae, L.K., Hubbard, A.L., and Tuma, P.L. (2003). Transcytotic efflux from early endosomes is dependent on cholesterol and glycosphingolipids in polarized hepatic cells. Mol. Biol. Cell *14*, 2689–2705.

Pelissier, A., Chauvin, J.P., and Lecuit, T. (2003). Trafficking through Rab11 endosomes is required for cellularization during Drosophila embryogenesis. Curr. Biol. *13*, 1848–1857.

Rahner, C., Stieger, B., and Landmann, L. (2000). Apical endocytosis in rat hepatocytes In situ involves clathrin, traverses a subapical compartment, and leads to lysosomes. Gastroenterology *119*, 1692–1707.

Rieder, C.L., Faruki, S., and Khodjakov, A. (2001). The centrosome in vertebrates: more than a microtubule-organizing center. Trends Cell Biol. *11*, 413–419.

Riggs, B., Rothwell, W., Mische, S., Hickson, G.R., Matheson, J., Hays, T.S., Gould, G.W., and Sullivan, W. (2003). Actin cytoskeleton remodeling during early Drosophila furrow formation requires recycling endosomal components nuclear-fallout and Rab11. J. Cell Biol. *163*, 143–154.

Rios, R.M., and Bornens, M. (2003). The Golgi apparatus at the cell centre. Curr. Opin. Cell Biol. *15*, 60–66.

Rolls, M.M., Albertson, R., Shih, H.P., Lee, C.Y., and Doe, C.Q. (2003). Drosophila aPKC regulates cell polarity and cell proliferation in neuroblasts and epithelia. J. Cell Biol. *163*, 1089–1098.

Schroeder, J.J., Crane, H.M., Xia, J., Liotta, D.C., and Merrill, A.H., Jr. (1994). Disruption of sphingolipid metabolism and stimulation of DNA synthesis by fumonisin B1. A molecular mechanism for carcinogenesis associated with Fusarium moniliforme. J. Biol. Chem. *269*, 3475–3481.

Spath, G.F., and Weiss, M.C. (1998). Hepatocyte nuclear factor 4 provokes expression of epithelial marker genes, acting as a morphogen in dedifferentiated hepatoma cells. J. Cell Biol. *140*, 935–946.

Tanaka, M., and Miyajima, A. (2003). Oncostatin M, a multifunctional cytokine. Rev. Physiol. Biochem. Pharmacol. *149*, 39–52.

Tuma, P.L., and Hubbard, A.L. (2003). Transcytosis: crossing cellular barriers. Physiol. Rev. *83*, 871–932.

Ueda, M., Graf, R., MacWilliams, H.K., Schliwa, M., and Euteneuer, U. (1997). Centrosome positioning and directionality of cell movements. Proc. Natl. Acad. Sci. USA *94*, 9674–9678.

van der Wouden, J.M., van IJzendoorn, S.C., and Hoekstra, D. (2002). Oncostatin M regulates membrane traffic and stimulates bile canalicular membrane biogenesis in HepG2 cells. EMBO J. *21*, 6409–6418.

van IJzendoorn, S.C., and Hoekstra, D. (1998). (Glyco)sphingolipids are sorted in sub-apical compartments in HepG2 cells: a role for non-Golgi-related intracellular sites in the polarized distribution of (glyco)sphingolipids. J. Cell Biol. *142*, 683–696.

van IJzendoorn, S.C., and Hoekstra, D. (1999a). Polarized sphingolipid transport from the subapical compartment: evidence for distinct sphingolipid domains. Mol. Biol. Cell *10*, 3449–3461.

van IJzendoorn, S.C., and Hoekstra, D. (1999b). The subapical compartment: a novel sorting centre? Trends Cell Biol. *9*, 144–149.

van IJzendoorn, S.C., and Hoekstra, D. (2000a). Polarized sphingolipid transport from the subapical compartment changes during cell polarity development. Mol. Biol. Cell *11*, 1093–1101.

van IJzendoorn, S.C., Maier, O., van Der Wouden, J.M., and Hoekstra, D. (2000). The subapical compartment and its role in intracellular trafficking and cell polarity. J. Cell Physiol. *184*, 151–160.

van IJzendoorn, S.C., and Mostov, K.E. (2000b). Connecting apical endocytosis to the intracellular traffic infrastructure in polarized hepatocytes. Gastroenterology *119*, 1791–1794.

van IJzendoorn, S.C., Zegers, M.M., Kok, J.W., and Hoekstra, D. (1997). Segregation of glucosylceramide and sphingomyelin occurs in the apical to basolateral transcytotic route in HepG2 cells. J. Cell Biol. *137*, 347–357.

Vermeer, P.D., Einwalter, L.A., Moninger, T.O., Rokhlina, T., Kern, J.A., Zabner, J., and Welsh, M.J. (2003). Segregation of receptor and ligand regulates activation of epithelial growth factor receptor. Nature. *422*, 322–326.

Wald, F.A., Figueroa, Y., Oriolo, A.S., and Salas, P.J. (2003). Membrane repolarization is delayed in proximal tubules after ischemia-reperfusion: possible role of microtubule-organizing centers. Am. J. Physiol. *285*, F230–F240.

Woo, R.A., and Poon, R.Y. (2003). Cyclin-dependent kinases and S phase control in mammalian cells. Cell Cycle *2*, 316–324.

Zhou, Q., He, Q., and Liang, L.J. (2003). Expression of p27, cyclin E and cyclin A in hepatocellular carcinoma and its clinical significance. World J. Gastroenterol. *9*, 2450–2454.

Zegers, M.M., and Hoekstra, D. (1997). Sphingolipid transport to the apical plasma membrane domain in human hepatoma cells is controlled by PKC and PKA activity: a correlation with cell polarity in HepG2 cells. J. Cell Biol. *138*, 307–321.